ENGINEERING DESIGN FILE

1. Project File No. _____ 2. Project/Task _____

3. Subtask _____

4. Title: Solids Characterization

5. Summary: In this EDF, the following conclusions are drawn on the INTEC tank farm solids:

- The solids settle leaving a clear supernate liquid above the solids layer. This was observed from LDUA footage of tanks WM-182, WM-183 and from the WM-182 sample in the RAL hot cell. The type of settling observed appeared to be flocculation sedimentation.
- Sonicated particle size distributions have a range of approximately 0.1 μm to 100 μm with a median at approximately 10 μm. Non-sonicated particle size distributions have a range of approximately 0.1 μm to 250 μm with a median at approximately 30 μm. This shift in particle size was interpreted to indicate the presence of flocculation and agglomeration. The non-sonicated case measured the size of the agglomerated particles under the specific flow conditions in the particle size analyzer. However, the sonicated case measured the size of the individual particles that form agglomerates.
- The solids particle density was found to be 2.0 g/ml on an air-dried basis. The sludge was found to contain 75% interstitial liquid and 25% air-dried solids in sludge by volume.
- Based on the process history of the tank farm, an estimated 45,000 gal (37 in heel height) is present in the tank farm. Approximately 15,000 gal (12 in heel height) of this sludge is already accounted in two of the 10 tanks (i.e. WM-182 and WM-183).
- The composition of the solids indicates a relatively large amount of Pu-238. Since Pu-238 is a TRU waste nuclide a large amount of waste (approximately 43,000 55-gallon drums) would be produced to treat the solids to the class C standard. Therefore, disposal of the solids as a LLW is, most likely, unrealistic. However, disposal as HLW or TRU waste should be further examined.

6. Distribution (complete package):

Distribution (summary package only):

7. Review (R) and Approval (A) Signatures: (Minimum reviews and approvals are listed. Additional reviews/approvals may be added as necessary.)

	R/A	Printed Name	Signature	Date
Author	R	Adam Poloski	Adam Poloski	9/19/00
Author	R	Michael Wilcox	Michael R. Wilcox	9/19/00
Technical Review	R	Dan Staiger	Dan Staiger	9/20/00
Requestor	A	William Landman	W H Landman	9/20/00

Contents

Summary 1

1 Introduction 5

2 Visual Data 5

3 Settling Type and Rate 12

4 Particle Size Distribution 15

5 Sludge Density Measurements 17

6 Solids Composition 18

7 Estimated Tank Farm Quantity 21

8 Waste Evaluation 22

9 Conclusions 27

References 28

A Appendix–Flocculation Theory 28

List of Figures

1 Inspection of Previous Sampling Locations (WM-182) 6
2 LDUA Sampler Moved Through The Sludge (WM-182) 7
3 Sludge Layer Oscillating with Sampler (WM-182) 7
4 WM-182 Sludge Sampling 8
5 WM-183 Sludge Sampling 9
6 Particles Floating on Clear Liquid (WM-182) 9
7 WM-183 Steam Jet 10
8 WM-183 Sludge Layer Topology 11
9 Tilting the WM-182 Hot Cell Sample 11
10 Settling Regimes 13
11 Accumulation Sedimentation and Flocculation Sedimentation 13
12 WM-182 Sludge Sample Settling Photographs 14
13 WM-182 Sludge Compression Settling Rate 15
14 WM-182 and WM-183 Particle Size Distributions 16
15 Horiba Sample Recirculation System 17
16 Density Comparison of Various Materials 18
17 Comparison of the Chemical Compositions of WM-182 and WM-183 19
18 Comparison of WM-182 and WM-183 TRU Waste Nuclides 26

List of Tables

1 Average Chemical Compositions of WM-182 and WM-183 20
2 Average Radionuclide Activities of WM-182 and WM-183 21
3 TCLP Test Results 21
4 Estimated Quantity of Tank Farm Sludge 22
5 Estimated Properties of Tank Farm Sludge in a Single Tank 23
6 Estimated Source Term of Tank Farm Sludge 23
7 Evaluation of Possible Final Waste Forms 25

1 Introduction

The purpose of this EDF is to compile the 1999 light duty utility arm (LDUA) solids sampling results for the purpose of designing a solid-liquid separation and treatment process. The information contained herein includes:

Visual data from the LDUA Images from the 1999 WM-182/183 sampling event are examined to gain a general insight of the physical properties of the solids.

Solids settling data A WM-182 sample was agitated and allowed to settle. Observations on the settling type and rate are discussed.

Particle size distributions The size of the solid particles is of great import for many solid-liquid separation operations. This section discusses the particle size distribution of WM-182 and WM-183 samples.

Particle density and sludge liquid content The solids chemical and radiochemical data are given on an air-died solids basis (i.e. air-dried particle density). In order to quantify the amount of solids and activity in each tank, one needs to know the air-dried solids density, bulk sludge volume, and percent of liquid present in the bulk sludge. These important physical properties are summarized from remote analytical laboratory (RAL) data and discussed.

Chemical and radiochemical data The samples gathered by the LDUA were sent to RAL for analysis. The results of the analysis are presented and discussed.

Estimate of the amount of solids in the entire INTEC tank farm A total amount of sludge present in the tank farm is predicted from previous process history of each tank.

Evaluation of the final treated solids waste form The previously discussed radiochemical and density data is used to find an estimated quanity of low-level (LLW), transuranic (TRU), or high-level waste (HLW) to be disposed.

2 Visual Data

While not based on strict empirical data, visual observations of the sludge material provide a general understanding of the behavior of the solids. We have a great amount of video footage from the LDUA during inspections and sampling. A few of the more interesting scenes pertaining to the surrogate solids effort from the WM-182,WM-183 video collection have been selected. These selections will be discussed and some conclusions will be drawn based on these photographs. The first set of images consists of the LDUA inspecting prior WM-182 sampling locations (see Figure 1). The photograph on the left shows one previous sample location. This sample location shows cracks on the surface of the sludge layer. The

cracks seem to indicate that the solids have solid-like properties. The photograph on the right shows a different sample location. This image shows the surface cracking similar to the other sample location. Therefore, this property is not localized. The right image also shows a distinct cylindrical shape at the sampling location. Since the LDUA sample port is cylindrical and the sample depression did not crumble to an angle of repose, this image also shows that the sludge layer acts solid-like in nature.

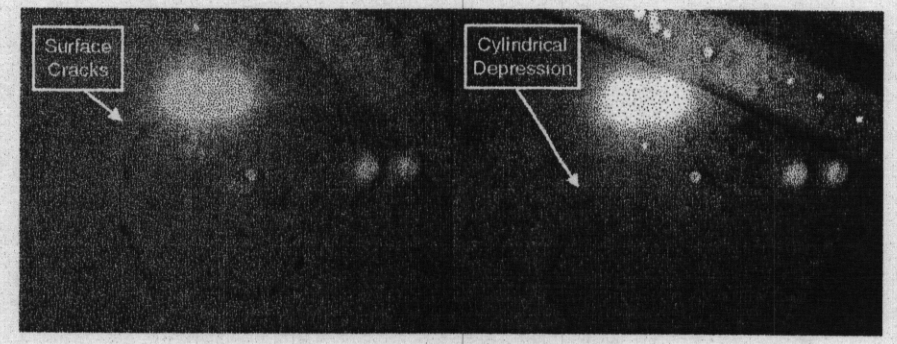

Figure 1: Inspection of Previous Sampling Locations (WM-182)

The second set of images consists of the LDUA inspecting a location where the sampler was previously moved through the WM-182 sludge layer (see Figure 2). The image on the right shows the original location where the sampler was placed in the sludge layer. Note the surface cracking is again present in this image. As the sampler was moved to the left, a wake developed behind the sampler. In this wake area, one can see relatively large solid clumps or agglomerates near the boundary of the wake area. Much smaller clumps are present in the center of the wake. This occurred because as the sampler was moved through the sludge layer large cracks would form near the wake boundary region. These cracks would eventually grow large enough to form large agglomerates. As these agglomerates move into the wake, larger shear rates are generated by the velocity gradient that break apart the agglomerates. Therefore, one could see the solid-like properties of the sludge under low shearing conditions at the wake boundary and fluid-like properties in the wake when the shear rates became large enough the break the agglomerates into smaller particles. Consequently, this material appears to act as a solid until a certain threshold is reached. At this point, the sludge begins to behave as a fluid. This is the definition of fluid dynamics property called a ***yield stress***. Sludges commonly possess this yield stress property.

Figure 3 shows a scene where the LDUA sampler was placed in the WM-182 sludge layer. As the sampler sat in the sludge layer, the LDUA mast was in the air above the tank. Gusts of wind oscillated the mast and in turn oscillated the sampler. As the sampler oscillated, an area of sludge around the sampler clearly oscillated with the sampler. While we could only observe the uppermost portion of the sludge layer, this situation demonstrates how the sludge layer possesses fluid-like properties.

Figure 4 shows a scene where the LDUA sampler was taking a sample from the WM-182

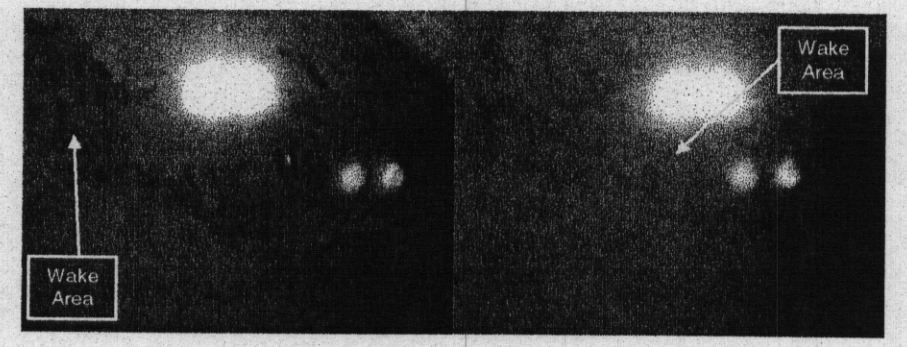

Figure 2: LDUA Sampler Moved Through The Sludge (WM-182)

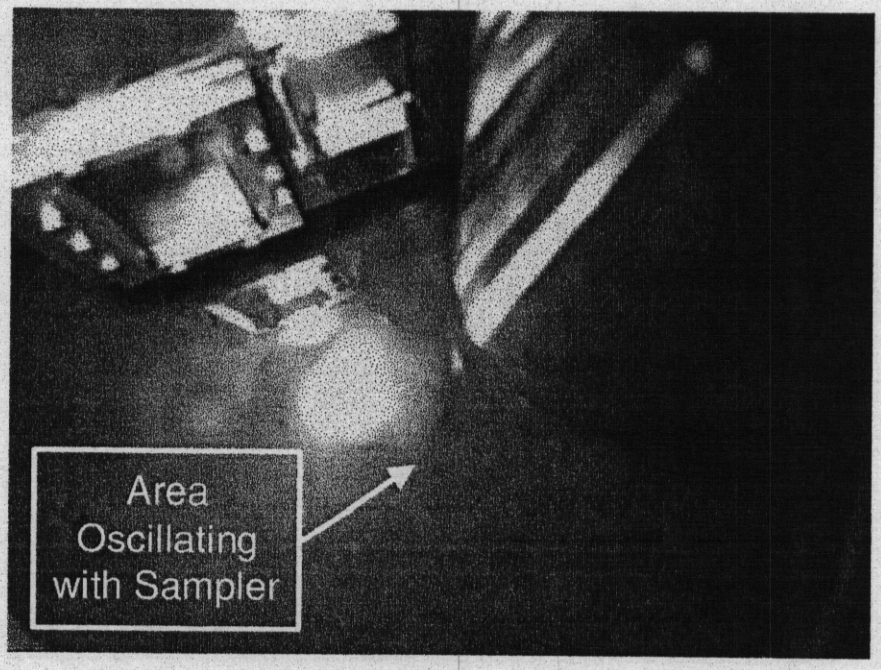

Figure 3: Sludge Layer Oscillating with Sampler (WM-182)

sludge layer. As the sampling began, surface cracks (as previously discussed) could be seen forming. Near the end of the of the sampling a relatively large amount of agitated solids could be seen billowing out near the sampler. This situation can be interpreted as follows:

- The surface cracks are forming due to low shear stresses under the yield stress threshold. As a result, the sludge particles act interdependently on each other and possess solid-like behavior.

- The billowy disturbance is generated due to larger shear forces that are above the yield stress threshold. As a result, the sludge particles act independently of each other and possess fluid-like behavior.

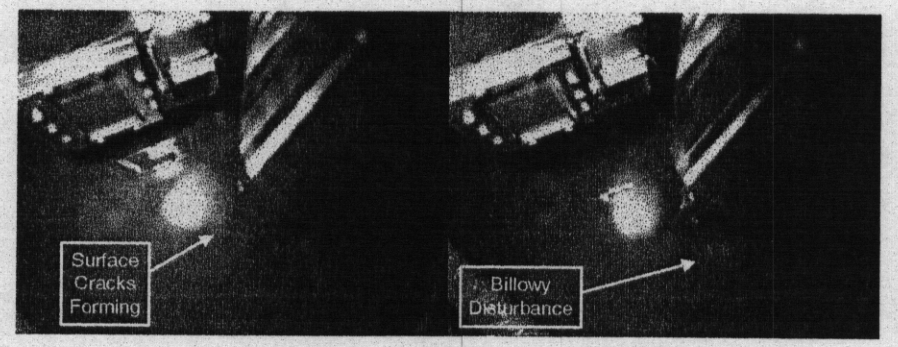

Figure 4: WM-182 Sludge Sampling

Figure 5 shows a scene where the LDUA sampler was taking a sample from the WM-183 sludge layer. The interesting feature in this scene is that while the WM-182 sludge layer was under a few inches of standing free liquid, the WM-183 sample location has no standing free liquid and the sludge layer is undersaturated. In this undersaturated condition the sludge layer appears to possess only fluid-like behavior. As the sampler is inserted, the sludge layer is pushed around the sampler in a fluid-like manner. When the sample is taken, no surface cracks form and the sludge could be likened to a thick mud.

Figure 6 shows the LDUA inspecting the WM-182 sludge. The images show particles floating on the surface of the standing liquid (see Figure 6). Under this layer of standing liquid one can see the settled sludge particles. This is interesting because previous sampling activities of tank liquid in the transfer lines have shown a relatively large amount of solids in the tank farm liquid. Many people have assumed these solids were due to suspended solids in the tank farm liquid. This image shows that the majority of the solids have settled out and some particles are suspended on the surface of the liquid due to surface tension. Consequently, the assumption that relatively large amounts of suspended undissolved solids ($3\ \frac{g\ UDS}{L}$)in the tank farm liquid could be in error. The UDS concentration measurements are from liquid samples taken as the tank farm liquid was transferred from one tank to another via steam jet eductor. Figure 7 shows the sludge layer around a steam jet eductor in

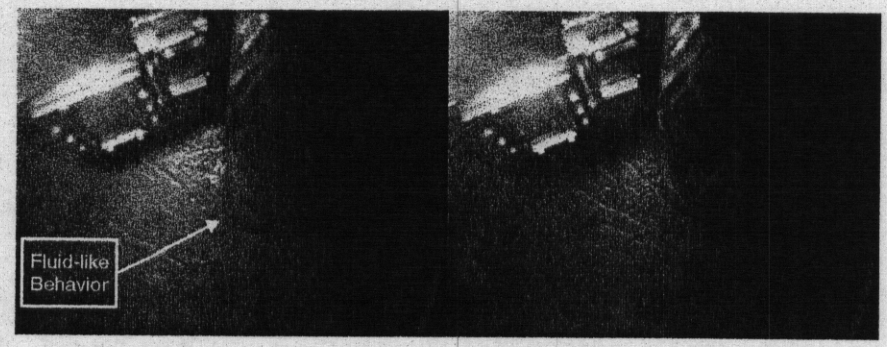

Figure 5: WM-183 Sludge Sampling

WM-183. As one can see, the steam jet not only transferred liquid but also entrained solids around the steam jet which may account for the large amount of "suspended" UDS.

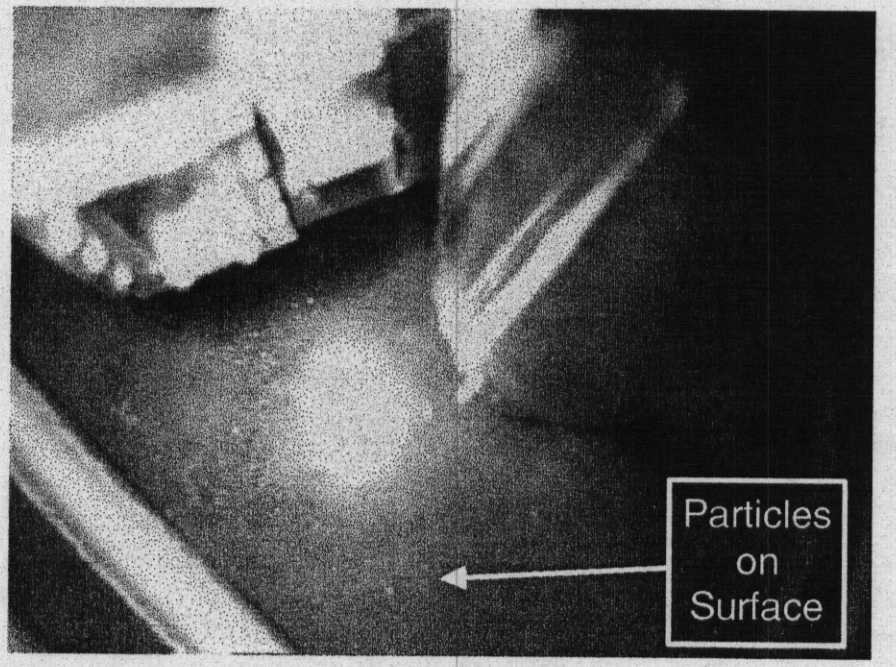

Figure 6: Particles Floating on Clear Liquid (WM-182)

One might argue that that once the depression around the steam jet is established the amount of entrained solids would be minimal. However, it seems that the required yield stress to agitate and move the solids is low and is met by simply transferring liquid from the tanks. Figure 8 shows the topology of the sludge layer in WM-183. After liquid was transferred from the tank, the topology of the sludge layer was significantly changed. This indicates that a significant amount of entrained solids could still be present after establishing

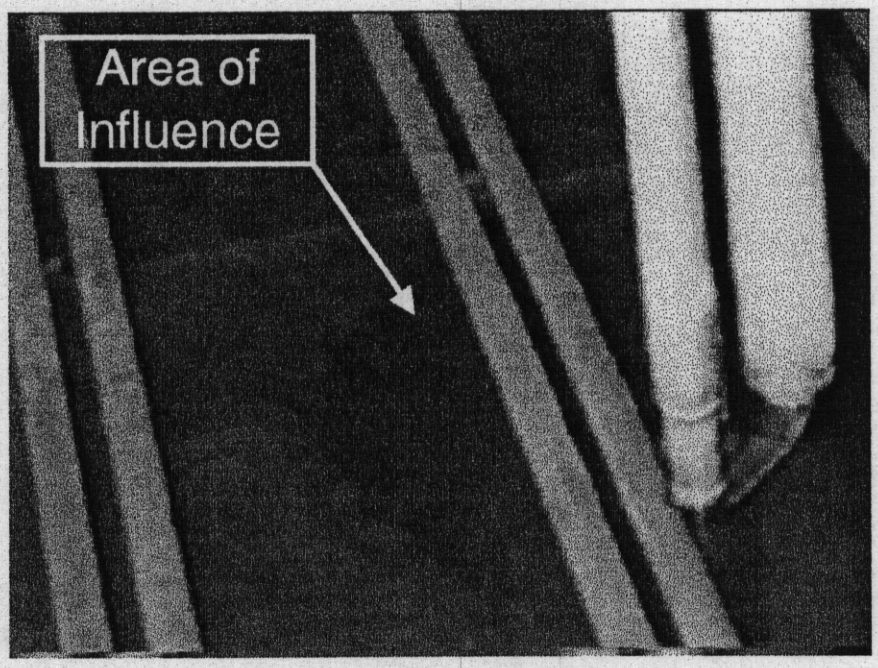

Figure 7: WM-183 Steam Jet

a depression around the steam jet. If one used a different method to transfer the liquid, such as slowly removing the liquid from the top, the UDS concentration should be minimized.

Besides LDUA footage, a WM-182 sample was taken and placed in the RAL hot cell. Figure 9 shows this sample as it is tilted to one side. As one can see, the clear liquid top layer is fluid-like and moves with gravity. The sludge layer, however, is solid-like and remains in its settled configuration. This again is evidence of a yield stress property. As the bottle was tilted quickly from one side to another, the sludge particle would break apart and become agitated and billowy, thus clouding the clear liquid layer.

In conclusion, the visual data we have discussed above provides evidence for the following conclusions:

- The solids are electrostaticly attracted to each other. This attraction provides the observed yield stress phenomenon and solid-like behavior (surface cracks, tilted bottle, etc.).
- The electrostatic attraction is relatively weak and once these forces have been broken the particles act in a fluid-like manner. This explains the observed change in sludge layer topology, the wake behind the sampler, and the billowy disturbances.
- This electrostatic attraction is the driving force behind flocculation. Further evidence of the sludge being a floc will be presented below. See Appendix A for a brief discussion on flocculation.

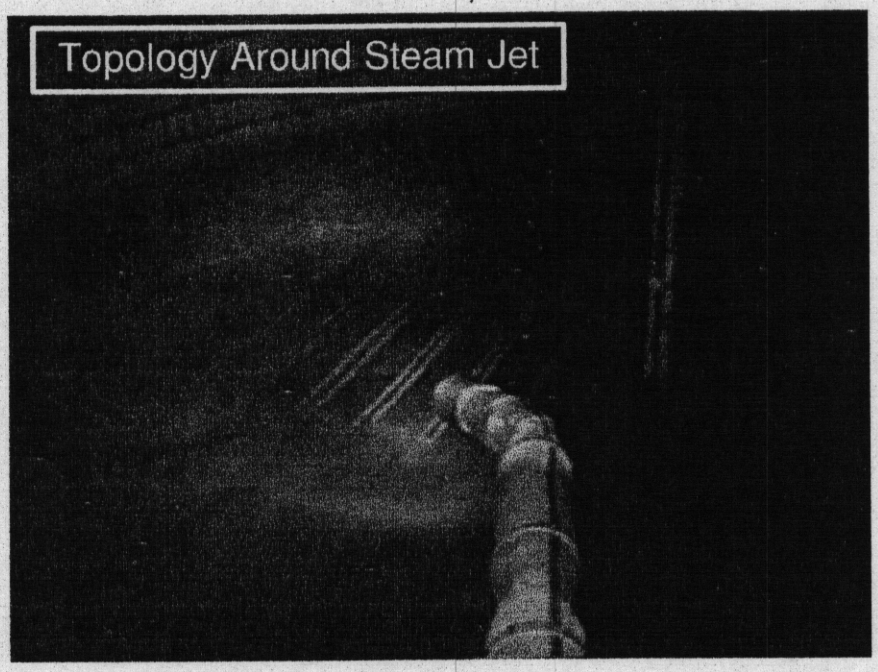

Figure 8: WM-183 Sludge Layer Topology

Figure 9: Tilting the WM-182 Hot Cell Sample

3 Settling Type and Rate

For certain types of solid/liquid separation operations, an understanding of the dynamics involved in settling is essential. Perry's Chemical Engineers' Handbook [3] has a general discussion of various settling regimes:

> At low concentrations, the type of settling encountered is called particulate settling. Regardless of their nature, particles are sufficiently far apart to settle freely. Faster settling particles may collide with slower settling ones and, if they do not cohere, continue downward at their own specific rate. Those that do cohere will form floccules of a larger diameter that will settle at a rate greater than that of individual particles.
>
> There is a gradual transition from particulate settling into the zone-settling regime, where the particles are constrained to settle as a mass. The principal characteristic of this zone is that the settling rate of the mass, as observed in batch tests, will be a function of the solids concentration (for any particular condition of flocculation, particle density, etc.).
>
> The solids concentration ultimately will reach a level at which particle descent is restrained not only by the hydrodynamic forces but partially by mechanical support from the particles below; therefore, the weight of the particles in mutual contact can influence the rate of sedimentation of those at lower levels. This compression, as it is termed, will result in further solids concentration because of compaction of the individual floccules and partial filling of the interfloc voids by the deformed floccules. Accordingly, the rate of sedimentation in the compression regime is a function of both the solids concentration and the depth of pulp in this particular zone. As indicated in Figure 10, granular, nonflocculent particles may reach their ultimate solids concentration without passing through this regime.

These types of settling are further discussed by Pierre and Ma [4]. In this paper, Pierre and Ma describe two types of settling, accumulation sedimentation, which is analogous to particulate settling, and flocculation sedimentation, which is analogous to zone/compression settling. These types of sedimentation are illustrated in Figure 11.

The WM-182 hot cell sludge sample was completely shaken and allowed to settle. Photographs were taken at various times after agitation. From the upper left photograph shown in Figure 12, one can see that we have a relatively high solids concentration. As a result, the degree of flocculation should be the determining factor in the type of settling that occurs. As time progresses after agitation, flocculation sedimentation or zone/compression settling is observed; indicating a relatively high degree of flocculation. From these pictures, we were able to scale the images to a similar sample bottle with a measured circumference and get the heights of the sample and settled sludge layer as a function of time. Nondimensionalizing the system involves using the following relation:

$$\text{Settled Solids Percent} = 100\% \times \frac{V_{sample} - V_t}{V_{sample} - V_\infty} \tag{1}$$

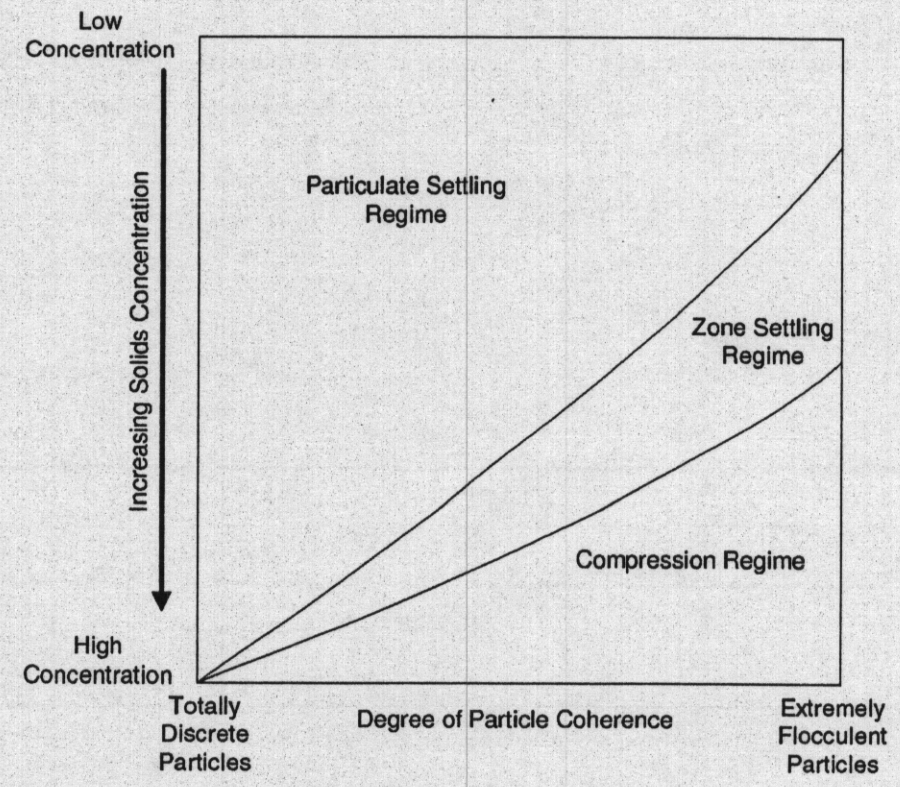

Figure 10: Settling Regimes

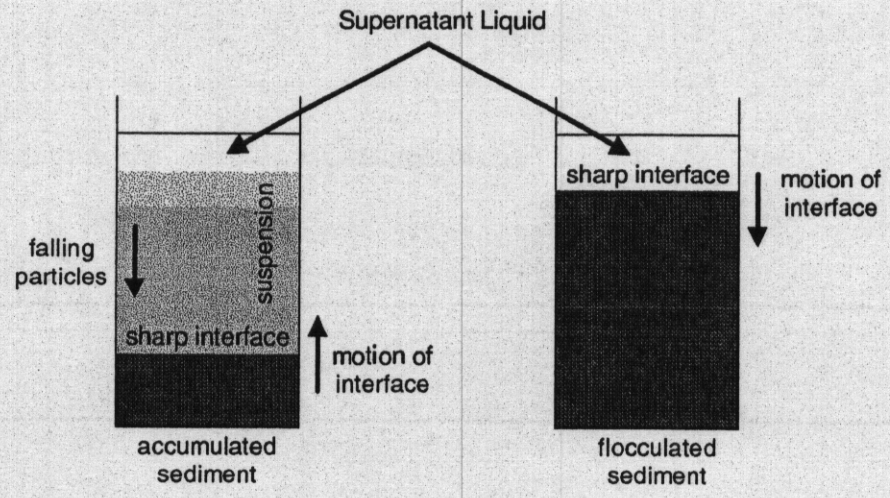

Figure 11: Accumulation Sedimentation and Flocculation Sedimentation

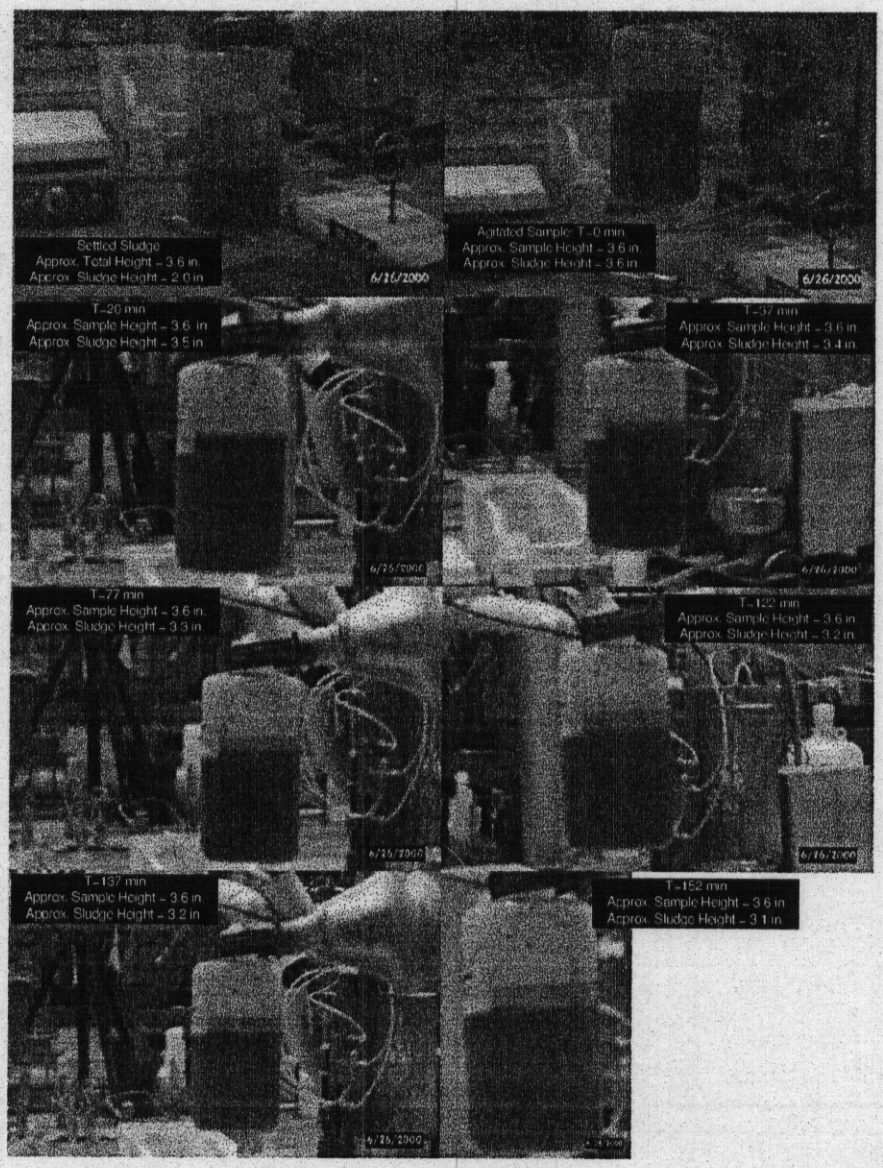

Figure 12: WM-182 Sludge Sample Settling Photographs

where,

V_{sample} is the total volume of the sample

V_t is the volume of the settled sludge layer at time t

V_∞ is the final settled volume of the sludge layer

From this equation, the plot shown in Figure 13 can be constructed. Note that there is no way to gauge the error involved in these data. Based on best professional judgment, a 20% error is assumed. A plot of the interface velocity as a function of time is shown in the same figure. From these photographs and plots, a slow flocculation sedimentation can be concluded.

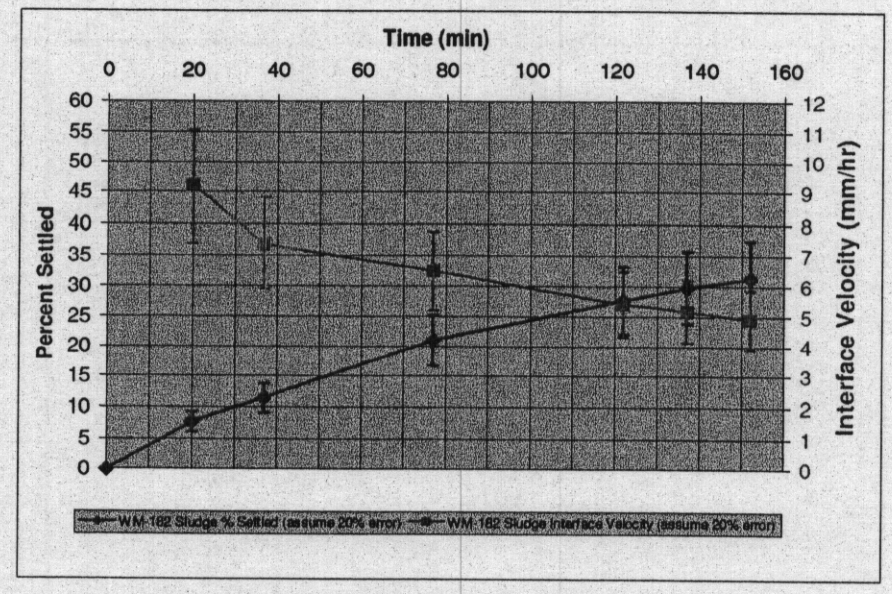

Figure 13: WM-182 Sludge Compression Settling Rate

4 Particle Size Distribution

A Horiba particle size analyzer was recently deployed in the RAL hot-cell. Several of the LDUA samples were analyzed using this particle size analyzer. The results of this analysis were compiled in "WM-182/183 Heel Slurry PSD Results Report" [7]. The particle size distribution (PSD) data in this report consists of two distributions for both WM-182 and WM-183. The first set of PSDs consists of data taken with the ultrasonic dispersion chamber turned off while the second set of data consists of PSDs with the ultrasonic dispersion chamber turned on. With the ultrasonic dispersion chamber off, the PSDs for both WM-182

and WM-183 were significantly shifted to the right (i.e. bigger particles, see Figure 14). This is expected since the ultrasonic dispersion chamber would disperse the floccules into their smaller "fundamental" component particles. For WM-182, the median sonicated particle size is approximately 8 μm. The WM-183 median sonicated particle size is approximately 12 μm. With the ultrasonic dispersion chamber off, the only thing to keep the particles from cohering to each other (i.e. flocculating) is the centrifugal recirculation pump (see Figure 15) which may or may not keep the system dispersed.

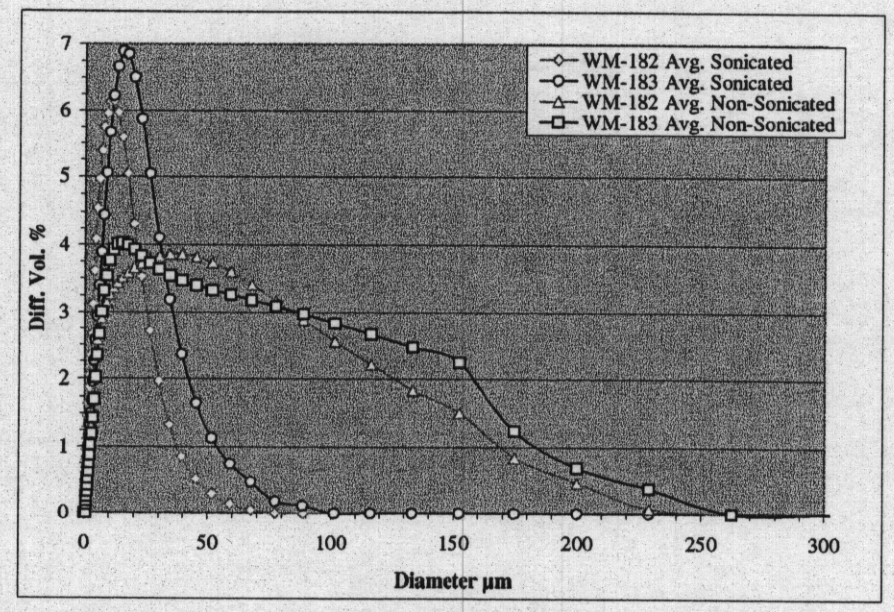

Figure 14: WM-182 and WM-183 Particle Size Distributions

Perry's Chemical Engineers' Handbook [3] has a general discussion of interparticle attraction and particle size:

> Figure 10 illustrates the relationship between solids concentration, interparticle cohesiveness, and the type of sedimentation that may exist. "Totally discrete" particles include many mineral particles (usually greater than 20 μm), salt crystals, and similar substances that have little tendency to cohere. "Flocculent" particles generally will include those smaller than 20 μm (unless present in a dispersed state due to surface charges), metal hydroxides, many chemical precipitates, and most organic substances other than true colloids.

If the "true" PSD is the non-sonicated case, the expected settling regime would be particulate settling due to the larger heavier particles and lack of cohesiveness. One would not expect the slow compression type settling that is observed. This again leads to the conclusion that flocculation could occur in the particle size analyzer and the sonicated PSD measures the smaller "fundamental" component particles in the sludge rather than floccules. Since these

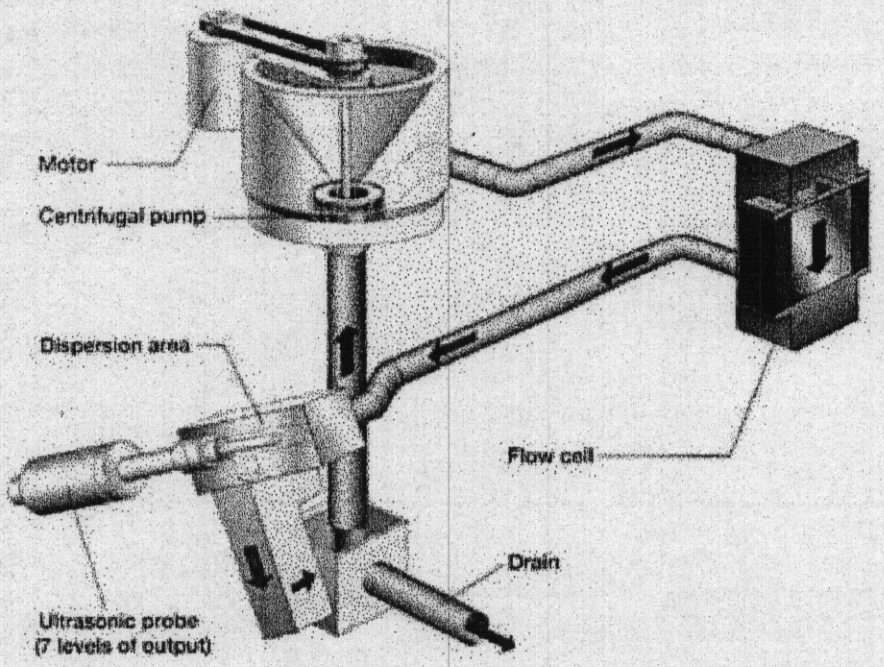

Figure 15: Horiba Sample Recirculation System

solids are believed to be formed by chemical precipitation in the tanks, the conclusion that the sludge is flocculent is supported by the quote given above at these particle sizes.

5 Sludge Density Measurements

The density of the solids are evaluated in an EDF written by Poloski [5]. The EDF reached the following conclusions:

- 75% interstitial liquid in sludge by volume
- 25% air-dried solids in sludge by volume
- 2.0 g/ml air-dried solids particle density

With the interstitial liquid SG (specific gravity) at approximately 1.2, the calculated tank farm sludge specific gravity would be 1.4.

Comparing these densities with other materials produces Figure 16. The solid materials shown in this graph are at the lower end of the density spectrum. Consequently, the sludge in the tank farm is relatively low-density. Since the oven-dried density of the solids was significantly higher than the air-dried density, the low density of the solids could be attributed to a large amount of hydrated water present in the crystalline structure of the particles.

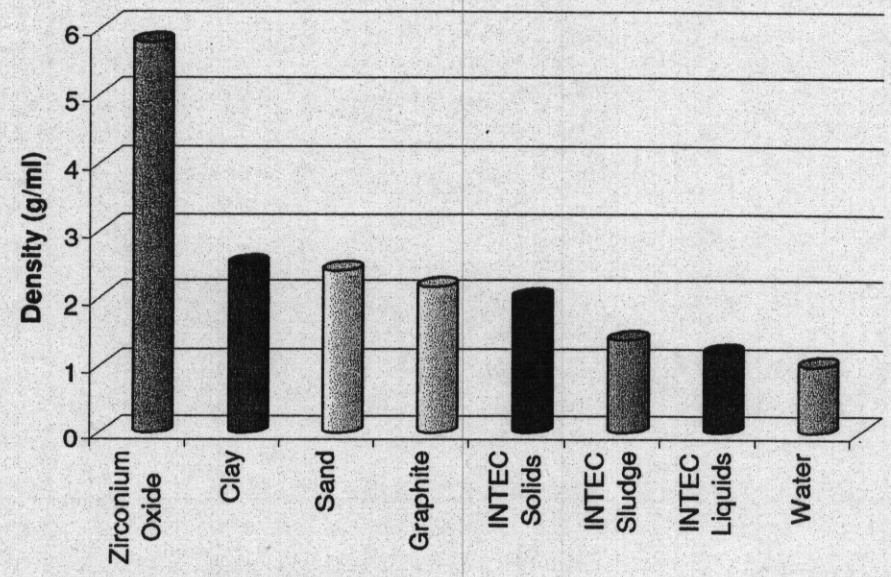

Figure 16: Density Comparison of Various Materials

Please note that these measurements involved air-drying the solids and then adding deionized water to reconstitute the sludge. Through this process, the interstitial liquid chemistry is significantly altered from the chemistry in the tank farm (e.g. pH, molar concentration of significant species, etc.). Changing the interstitial liquid chemistry can, in turn, change the solids surface chemistry. Changing the surface chemistry alters the so-called *zeta potential*, which is an indicator of how the solid particles interact with each other. Ultimately, the solids packing and interstitial liquid fraction can be significantly altered by the chemistry of the interstitial liquid (the particle density measurements should be unaffected). Even with this potential source of error, these RAL data are the best available tank farm sludge density data.

Changing the liquid phase composition can also alter settling type and rate. When the solids are washed (via washball) and transported to another tank, the ionic composition of the liquid should be significantly diluted. Further investigation on diluting the liquid phase and changes of settling type and rate of the solids should be a priority.

6 Solids Composition

The LDUA samples have also been analyzed for various chemical constituents and radionuclides. These analyses were performed on an air-dried mass basis. Therefore, the density data discussed above should be used in conjunction with the data presented in this section.

The averaged metal and anion data are presented in Table 1. These data are taken from a letter written by Millet [2]. The third column was added to provide the maximum average value between tanks WM-182 and WM-183. Species with the higher compositions

are presented on a mass percent basis in Figure 17. One should note that nitrates are typically soluble in water. Therefore, the higher nitrate compositions present in the solids are surprising. One would tend to think that these nitrate readings result from the interstitial liquid rather than actually being present in the solid crystalline matrix. The nitrate ions may have been absorbed on the surface of the solid particles or present in particle pores. It may also be possible that the interstitial liquid was not completely removed during sample preparation. Also, note that the chemical speciation listed here only accounts for 43.8% for WM-182 and 48.6% for WM-183 (by mass). The remaining mass most likely consists of unaccounted oxygen and hydrated water. From discussion with laboratory technicians who performed the work, the solids were not oven-dried prior to analysis. The oven-dried density of WM-183 solids was calculated as 5.7 $rm\frac{g}{ml}$ while the air-dried particle density was calculated as 2.0 $\frac{g}{ml}$. From this large difference in density, it is apparent that a large amount of hydrated water exists in the solids.

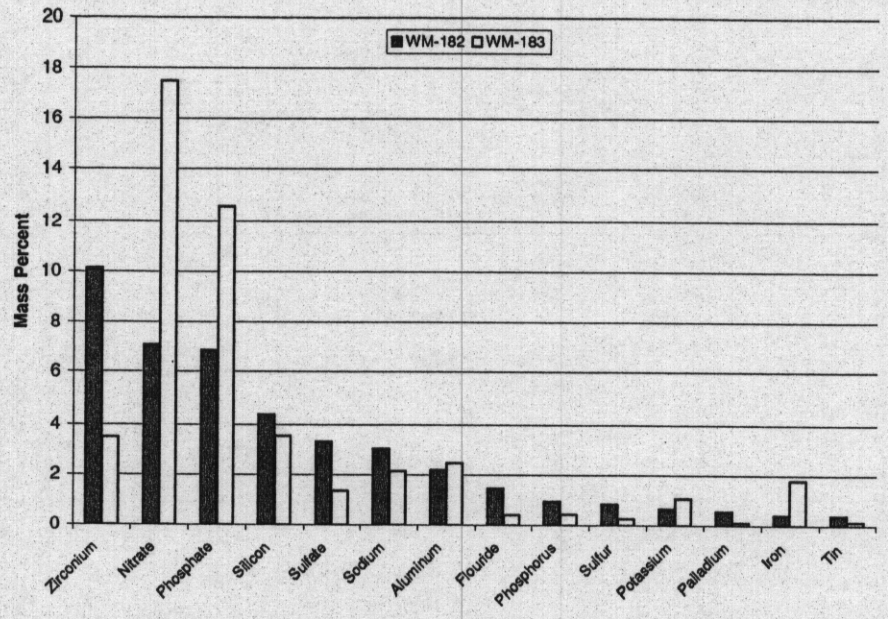

Figure 17: Comparison of the Chemical Compositions of WM-182 and WM-183

Millet also supplied the averaged radionuclide activities for WM-182 and WM-183. These data are presented in Table 2. A cursory evaluation of these data reveals a wide degree of variability between the activities in WM-182 and WM-183. Generally speaking, the WM-182 sample has the higher activity. A more thorough examination of these radionuclide data will be performed in Section 8.

Lastly, TCLP tests were performed on the solids. The TCLP results from WM-182 and WM-183 reveal that the solids failed the Cadmium, Chromium, Lead, and Mercury leaching tests (see Table 3). Consequently, the solids possess the following RCRA waste codes:

- D006, D007, D008, D009

Chemical Analyses						
Component	**Symbol**	**Units**	**WM-182 Value**	**WM-183 Value**	**Maximum 182/183 Value**	**Max % Difference**
Aluminum	Al	mg/kg	2.19E+04	2.49E+04	2.49E+04	14%
Antimony	Sb	mg/kg	<1.45E+01	3.20E+01	3.20E+01	--
Arsenic	As	mg/kg	2.81E+02	5.56E+01	2.81E+02	406%
Barium	Ba	mg/kg	1.27E+02	2.36E+01	1.27E+02	437%
Beryllium	Be	mg/kg	<1.16E+00	<8.88E-01	<1.16E+00	--
Boron	B	mg/kg	1.50E+02	1.82E+02	1.82E+02	21%
Cadmium	Cd	mg/kg	3.25E+02	1.42E+02	3.25E+02	128%
Calcium	Ca	mg/kg	1.77E+03	1.87E+03	1.87E+03	6%
Cerium	Ce	mg/kg	<2.14E+01	2.00E+01	<2.14E+01	--
Cesium	Cs	mg/kg	4.20E+01	9.29E+00	4.20E+01	352%
Chloride	Cl	mg/kg	2.02E+03	1.31E+03	2.02E+03	54%
Chromium	Cr	mg/kg	5.52E+02	9.49E+02	9.49E+02	72%
Cobalt	Co	mg/kg	<9.25E+00	9.33E+00	9.33E+00	--
Copper	Cu	mg/kg	2.98E+02	1.66E+02	2.98E+02	80%
Flouride	F	mg/kg	1.48E+04	4.37E+03	1.48E+04	238%
Gadolinium	Gd	mg/kg	5.26E+01	1.70E+02	1.70E+02	224%
Iron	Fe	mg/kg	4.48E+03	1.80E+04	1.80E+04	301%
Lead	Pb	mg/kg	3.69E+02	2.74E+02	3.69E+02	35%
Lithium	Li	mg/kg	5.94E+00	4.00E+00	5.94E+00	49%
Magnesium	Mg	mg/kg	4.10E+02	4.34E+02	4.34E+02	6%
Manganese	Mn	mg/kg	5.65E+02	7.40E+02	7.40E+02	31%
Mercury	Hg	mg/kg	3.10E+02	3.24E+02	3.24E+02	4%
Molybdenum	Mo	mg/kg	2.50E+03	6.94E+02	2.50E+03	260%
Nickel	Ni	mg/kg	3.09E+02	4.17E+02	4.17E+02	35%
Niobium	Nb	mg/kg	1.28E+03	6.23E+02	1.28E+03	105%
Nitrate	NO_3	mg/kg	7.07E+04	1.75E+05	1.75E+05	147%
Palladium	Pd	mg/kg	5.77E+03	1.44E+03	5.77E+03	299%
Phosphate	PO_4	mg/kg	6.84E+04	1.26E+05	1.26E+05	84%
Phosphorus	P	mg/kg	9.59E+03	4.61E+03	9.59E+03	108%
Potassium	K	mg/kg	7.05E+03	1.09E+04	1.09E+04	55%
Ruthenium	Ru	mg/kg	8.29E+02	2.13E+03	2.13E+03	156%
Selenium	Se	mg/kg	9.11E+01	<1.28E+01	9.11E+01	--
Silicon	Si	mg/kg	4.39E+04	3.53E+04	4.39E+04	24%
Silver	Ag	mg/kg	6.47E+01	2.20E+02	2.20E+02	240%
Sodium	Na	mg/kg	3.04E+04	2.14E+04	3.04E+04	42%
Strontium	Sr	mg/kg	<9.25E+00	1.07E+01	1.07E+01	--
Sulfate	SO_4	mg/kg	3.32E+04	1.36E+04	3.32E+04	144%
Sulfur	S	mg/kg	8.74E+03	2.85E+03	8.74E+03	207%
Thallium	Tl	mg/kg	<1.68E+01	<1.36E+01	<1.68E+01	--
Tin	Sn	mg/kg	4.07E+03	1.47E+03	4.07E+03	178%
Titanium	Ti	mg/kg	6.50E+02	7.11E+02	7.11E+02	9%
Uranium	U	mg/kg	<4.62E+01	1.93E-01	4.62E+01	--
Vanadium	V	mg/kg	1.33E+01	1.07E+01	1.33E+01	25%
Zinc	Zn	mg/kg	1.79E+02	1.48E+02	1.79E+02	21%
Zirconium	Zr	mg/kg	1.01E+05	3.49E+04	1.01E+05	191%
Total	tot	mass %	43.8%	48.6%	--	--

Table 1: Average Chemical Compositions of WM-182 and WM-183

Radiochemical Analyses						
Component	Symbol	Units	WM-182 Value	WM-183 Value	Maximum 182/183 Value	Max % Difference
Americium 241	Am-241	mCi/g	8.46E-04	2.45E-04	8.46E-04	246%
Antimony 125	Sb-125	mCi/g	5.77E-02	2.90E-03	5.77E-02	1890%
Cesium 134	Cs-134	mCi/g	6.64E-03	5.89E-04	6.64E-03	1027%
Cesium 137	Cs-137	mCi/g	4.50E+00	8.68E-01	4.50E+00	419%
Cobalt 60	Co-60	mCi/g	2.14E-04	not reported	2.14E-04	--
Curium 244	Cm-244	mCi/g	2.84E-06	not reported	2.84E-06	--
Europium 154	Eu-154	mCi/g	1.48E-03	7.56E-04	1.48E-03	95%
Iodine 129	I-129	mCi/g	<2.22E-07	<9.03E-08	2.22E-07	--
Neptunium 237	Np-237	mCi/g	1.68E-06	1.76E-06	1.76E-06	5%
Plutonium 238	Pu-238	mCi/g	1.93E-02	4.00E-03	1.93E-02	383%
Plutonium 239	Pu-239	mCi/g	1.47E-03	1.25E-03	1.47E-03	17%
Strontium 90*	Sr-90	mCi/g	2.29E-01	1.82E-01	2.29E-01	26%
Technetium 99	Tc-99	mCi/g	2.63E-03	3.29E-05	2.63E-03	7902%
Tritium	H-3	mCi/g	1.15E-05	not reported	1.15E-05	--
Uranium 234	U-234	mCi/g	<2.4E-06	<3.3E-06	3.30E-06	--
Uranium 235	U-235	mCi/g	2.61E-07	9.29E-08	2.61E-07	181%
Uranium 236	U-236	mCi/g	3.05E-07	<3.4E-08	3.05E-07	--
Uranium 238	U-238	mCi/g	3.83E-08	6.91E-08	6.91E-08	80%

* Reported as total Sr

Table 2: Average Radionuclide Activities of WM-182 and WM-183

TCLP Analyses							
EPA HW Code	Component	Symbol	Units	WM-182 Value	WM-183 Value	Maximum 182/183 Value	RCRA Limit
D004	Arsenic	As	mg/L	0.022	0.022	0.022	5
D005	Barium	Ba	mg/L	0.24	0.78	0.78	100
D006	Cadmium	Cd	mg/L	*2.2*	*5.8*	*5.8*	1
D007	Chromium	Cr	mg/L	1.9	*25*	*25*	5
D008	Lead	Pb	mg/L	0.0	*6.8*	*6.8*	5
D009	Mercury	Hg	mg/L	*3.1*	*17.3*	*17.3*	0.2
D010	Selenium	Se	mg/L	0.018	0.018	0.018	1
D011	Silver	Ag	mg/L	0.046	0.70	0.70	5

Does Not Exhibit Associated RCRA Toxicity Characteristic
Exhibits Associated RCRA Toxicity Characteristic

Table 3: TCLP Test Results

7 Estimated Tank Farm Quantity

Currently, the approximate quantity of sludge in tanks WM-182, WM-183 and WM-188 is known through LDUA video footage. Based on discussions with Ed Wagner, the quantities of solids in other INTEC tank farm tanks have been estimated. The basis of this estimation is the quantities of solids in tanks WM-182, WM-183 and WM-188 and knowledge of their process history. With knowledge of the process history of the other tanks in the tank farm, one can extrapolate for the quantities of solids in tanks other than WM-182, WM-183 and

WM-188. The results of this extrapolation are shown in Table 4 and discussed below:

- This calculation assumes 75.0% (vol.) interstitial liquid in the sludge.
- This calculation assumes a particle density of 2.0 g/ml.
- Cooling coil volumes are assumed to be negligible.
- Tanks WM-180, WM-181, WM-184, WM-185, and WM-186 are expected to have solids levels near the value of WM-182 (4"). After washing, some of the solids on the tank walls are assumed to be removed and produce an additional 1/2" layer on the bottom.
- Tanks WM-187, and WM-189 are expected to have solids levels near the value of WM-188 (1/4"). After washing, some of the solids on the tank walls are assumed to be removed and produce an additional 1/4" layer.
- From video footage tank WM-183 had a sludge height of 8". After washing, the solids on the walls are assumed to be removed and produce an additional 1/2" layer.

Estimated Solids Quantities (Inches of sludge)			
Tank	Sludge Height	Sludge on Walls	Total Sludge
WM-180 (like WM-182)	4.00	0.50	4.5
WM-181 (like WM-182)	4.00	0.50	4.5
WM-182	4.00	0.50	4.5
WM-183	8.00	0.50	8.5
WM-184 (like WM-182)	4.00	0.50	4.5
WM-185 (like WM-182)	4.00	0.50	4.5
WM-186 (like WM-182)	4.00	0.50	4.5
WM-187 (like WM-188)	0.25	0.25	0.5
WM-188	0.25	0.25	0.5
WM-189 (like WM-188)	0.25	0.25	0.5
WM-190 (empty)	0.00	0.00	0.0
Total	32.75	4.25	37.0

Table 4: Estimated Quantity of Tank Farm Sludge

If this quantity of sludge is transferred to one tank, the sludge layer would have the properties shown in Table 5

8 Waste Evaluation

This section will provide a basic investigation into the three basic waste classifications (HLW, TRU and LLW) that the tank farm solids may be classified. The first step in this investigation is to find the source term for the solids. If the maximum WM-182 and WM-183

Tank Conditions (All Sludge in One Tank)	
Particle SG	2.0
Area of Bottom of tank	1,963 ft^2
Depth of Sludge Layer	37.0 in
Volume of Sludge Layer	6,054 ft^3
Volume of Sludge Layer	45,291 gal
Volume of Sludge Layer	171,452 l
Liquid Fraction	0.75
Volume of Solids	42,863 l
Volume of Liquid	128,589 l
Mass of Solids	85,726 kg

Table 5: Estimated Properties of Tank Farm Sludge in a Single Tank

Component	Symbol	WM-182 Basis	WM-183 Basis	Max. Source Term	units
Americium 241	Am-241	7.25E+01	2.10E+01	7.25E+01	Ci
Antimony 125	Sb-125	4.94E+03	2.48E+02	4.94E+03	Ci
Cesium 134	Cs-134	5.69E+02	5.05E+01	5.69E+02	Ci
Cesium 137	Cs-137	3.86E+05	7.44E+04	3.86E+05	Ci
Cobalt 60	Co-60	1.84E+01		1.84E+01	Ci
Curium 244	Cm-244	2.43E-01		2.43E-01	Ci
Europium 154	Eu-154	1.27E+02	6.48E+01	1.27E+02	Ci
Iodine 129	I-129	1.90E-02	7.74E-03	1.90E-02	Ci
Neptunium 237	Np-237	1.44E-01	1.51E-01	1.51E-01	Ci
Plutonium 238	Pu-238	1.66E+03	3.43E+02	1.66E+03	Ci
Plutonium 239	Pu-239	1.26E+02	1.08E+02	1.26E+02	Ci
Strontium 90*	Sr-90	1.97E+04	1.56E+04	1.97E+04	Ci
Technetium 99	Tc-99	2.26E+02	2.82E+00	2.26E+02	Ci
Tritium	H-3	9.87E-01		9.87E-01	Ci
Uranium	U	3.96E+00	1.66E-02	3.96E+00	kg
Uranium 234	U-234	2.06E-01	2.83E-01	2.83E-01	Ci
Uranium 235	U-235	2.24E-02	7.96E-03	2.24E-02	Ci
Uranium 236	U-236	2.61E-02	2.91E-03	2.61E-02	Ci
Uranium 238	U-238	3.28E-03	5.92E-03	5.92E-03	Ci

* Reported as total Sr

Table 6: Estimated Source Term of Tank Farm Sludge

concentrations are used for all 37 inches of solids, the air-dried density data discussed previously can be used to gain an initial source term. This source term to be disposed is shown in Table 6.

If the solids are deemed HLW, they would need to be disposed at the National Repository (i.e. Yucca Mountain). The preferred waste form for the National Repository is glass. In this instance, we would want to produce a glass with a maximum waste loading. After discussions with Rod Kimmitt, a glass waste loading of 35% seems reasonable as vitrification product (with a glass SG of 2.6).

If the solids are deemed not to be HLW, then TRU waste is the next level on the hierarchy. TRU waste can be disposed at WIPP, however, free liquids must not be present in the final waste form. Therefore, three different scenarios can be envisioned for solids waste forms to be disposed at WIPP:

- TRU Glass–again, assume 35% waste loading and glass SG of 2.6
- TRU Grout–assume 35% waste loading and grout SG of 2.1
- Dried TRU Solids–assume 100% waste loading and 1.0 g/ml average centrifuged solids bulk density [5]

Finally a LLW form needs to be considered. The likely form for LLW would be grout. Again, the grout SG is assumed to be 2.1. The waste loading is then calculated as the maximum value to reach Class C.

Based on these assumptions, the calculations shown in Table 7 can be performed. These cursory calculations show that nearly 43,000 55-gallon drums would need to be disposed as Class C if the solids were treated as LLW. This large number of drums presents an unrealistic and costly disposal constraint. Therefore, the LLW disposal option should not be considered viable. Furthermore, the radionuclide that represents the bottleneck in this disposal option is Pu-238. Since Pu-238 is a TRU-waste nuclide, the difference in the quantity of waste generated at Class C and at TRU-waste (i.e. the range of the greater than Class C designation) is very small. Therefore, disposal as a greater than class C waste at the National Repository would not be realistic.

An examination of the TRU waste nuclides on a tank by tank basis shows that WM-183 has a much lower TRU waste nuclide activity than WM-182 (see Figure 18). However, both WM-182 and WM-183 solids exceed the 100 nCi/g limit by several orders of magnitude.

Note that the National Repository or WIPP may still not accept these quantities of HLW/TRU-waste. Dose, fissile-gram-equivalent (FGE), and Pu-239 equivalent activity (PE-Ci) calculations need to be performed and satisfactorily meet the requirements set in the various waste acceptance criteria. Consequently, the assumed waste loadings could be altered to satisfy these requirements. Please note that the current WM-182 and WM-183 data does not include enough data to perform the calculations discussed above. Estimations of the lacking data have been calculated by Staiger [6]. However, the scope of this EDF is to report established, measured data and use of estimated data should be considered on a case by case basis.

Waste Form	HLW Glass	TRU Glass	TRU Grout	TRU Solids	LLW Grout	Units
Assumed Waste Loading	35	35	35	100	0.458	mass %
Waste Form SG	2.6	2.6	2.1	1.0	2.1	--
Waste Mass	244,932	244,932	244,932	85,726	18,717,513	kg
Waste Volume	94	94	117	84	8,913	m^3
Number of 0.7 m^3 Glass Canisters	135	135	167	121	12,734	--
Number of 55-gallon Drums	453	453	561	405	42,809	--
Radionuclide	Concentration					
Americium 241	296	296	296	846	4	nCi/g
Curium 244	0.99	0.99	0.99	2.84	0.0130	nCi/g
Neptunium 237	0.61	0.61	0.61	1.76	0.0080	nCi/g
Plutonium 238	6,764	6,764	6,764	19,324	89	nCi/g
Plutonium 239	514	514	514	1,468	7	nCi/g
TRU Waste Concentration	7,575	7,575	7,575	21,642	99.12	nCi/g
Cesium 137	4,097	4,097	3,309	4,581	43	Ci/m^3
Cobalt 60	0.20	0.20	0.16	0.22	0.0021	Ci/m^3
Iodine 129	0.00020	0.00020	0.00016	0.00023	0.0000021	Ci/m^3
Strontium 90*	209	209	169	233	2.21	Ci/m^3
Technetium 99	2.40	2.40	1.93	2.68	0.025	Ci/m^3
Tritium	0.010	0.010	0.0085	0.0117	0.00011	Ci/m^3
Short-Lived Class A Sum of Fractions Number	--	--	--	--	98.44	--
Long-Lived Class A Sum of Fractions Number	--	--	--	--	10.00	--
Short-Lived Class B Sum of Fractions Number	--	--	--	--	0.999	--
Long-Lived Class B Sum of Fractions Number	--	--	--	--	9.997	--
Short-Lived Class C Sum of Fractions Number	--	--	--	--	0.010	--
Long-Lived Class C Sum of Fractions Number	--	--	--	--	1.000	--
Waste Determination	HLW	TRU	TRU	TRU	Class C	--

* Reported as total Sr

Table 7: Evaluation of Possible Final Waste Forms

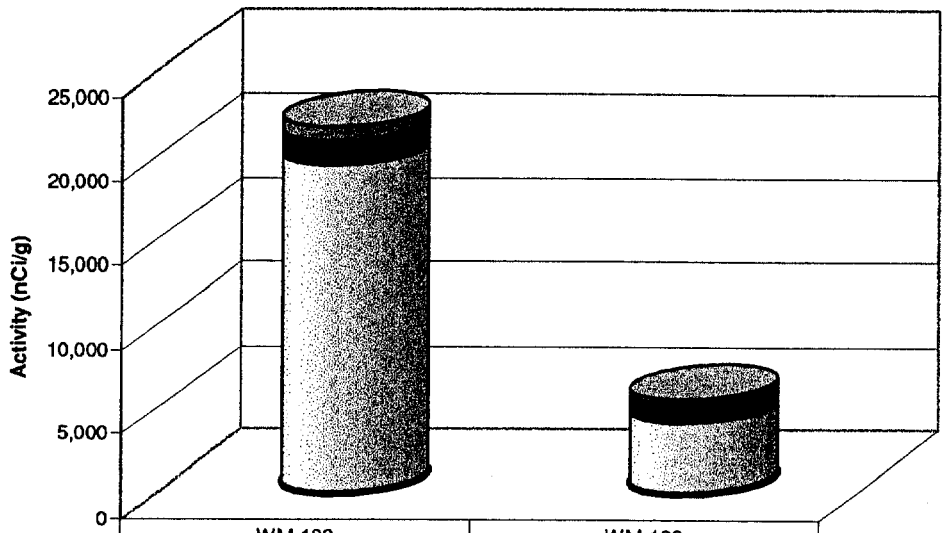

	WM-182	WM-183
Np-237	2	2
Cm-244	3	0
Am-241	846	245
Pu-239	1,468	1,254
Pu-238	19,324	4,000
TRU/LLW 100 nCi/g Limit	100	100

Figure 18: Comparison of WM-182 and WM-183 TRU Waste Nuclides

9 Conclusions

In this EDF, the following conclusions are drawn on the INTEC tank farm solids:

- The solids settle leaving a clear supernate liquid above the solids layer. This was observed from LDUA footage of tanks WM-182, WM-183 and from the WM-182 sample in the RAL hot cell. The type of settling observed appeared to be flocculation sedimentation.

- Changing the liquid phase composition can alter settling type and rate. When the solids are washed (via washball) and transported to another tank, the ionic composition of the liquid should be significantly diluted. Further investigation on diluting the liquid phase and changes of settling type and rate of the solids should be a priority.

- Sonicated particle size distributions have a range of approximately 0.1 μm to 100 μm with a median at approximately 10 μm. Non-sonicated particle size distributions have a range of approximately 0.1 μm to 250 μm with a median at approximately 30 μm. This shift in particle size was interpreted to indicate the presence of flocculation and agglomeration. The non-sonicated case measured the size of the agglomerated particles under the specific flow conditions in the particle size analyzer. However, the sonicated case measured the size of the individual particles that form agglomerates.

- The solids particle density was found to be 2.0 g/ml on an air-dried basis. The sludge was found to contain 75% interstitial liquid and 25% air-dried solids in sludge by volume.

- Based on the process history of the tank farm, an estimated 45,000 gal (37 in) is present in the tank farm. Approximately 15,000 gal (12 in) of this sludge is already accounted in two of the 10 tanks (i.e. WM-182 and WM-183).

- The composition of the solids indicates a relatively large amount of Pu-238. Since Pu-238 is a TRU waste nuclide a large amount of waste (approximately 43,000 drums) would be produced to treat the solids to the class C standard. Therefore, disposal of the solids as a LLW is unrealistic. However, disposal as HLW or TRU waste should be further examined.

References

[1] N.M. Gric and B.D. Lric. Flocculation: Theory and application. *Mine and Quarry Journal*, May 1978.

[2] C. B. Millet. WM-182 and WM-183 Tank Sampling Summary. Interoffice Memorandum, July 2000. MIL-03-00, Memo to J. T. Beck.

[3] Perry and Green. *Perry's Chemical Engineers' Handbook.* McGraw Hill, New York, 6th edition, 1984.

[4] A.C. Pierra and K. Ma. DLVO theory and clay aggregate architectures formed with $AlCl_3$. *Journal of the European Ceramic Society*, 19:1615–1622, 1999.

[5] A. P. Poloski. INTEC Tank Farm Sludge Density Measurements/Calculations. Technical Report EDF 15722-040, Idaho National Engineering & Environmental Laboratory, 2000.

[6] M Daniel Staiger. Estimate for Bounding Tank. Interoffice Memorandum, March 2000. MDS-05-00, Memo to Keith Quigley.

[7] T. A. Batcheller. WM-182/183 Heel Slurry PSD Results Report (Draft), 2000.

A Appendix–Flocculation Theory

Since the fundamental concept behind surrogate development involves flocculation, the following provides a brief introduction to some basic concepts of colloids, coagulation, and flocculation [1].

Many minerals, some organic pollutants, proteinaceous materials, some algae, and some bacteria are suspended in water as very small particles. Such particles, which have characteristics of both species in solution and larger particles in suspension, range in diameter from about 0.001 μm to about 1 μm. These particles are classified as colloids. Colloids may be classified as hydrophilic colloids, hydrophobic colloids, or association colloids. Hydrophobic colloids interact to a lesser extent with water and are stable because of their positive or negative electrical charges. The charged surface of the colloidal particle and the counter-ions that surround it compose an electrical double layer (adsorbed-ion layer and counter-ion layer), which causes the particles to repel each other. Colloidal particles are thus prevented from aggregating. Hydrophobic colloids are usually caused to settle from suspension by the addition small quantities of salts that contribute ions to solution. Clay particles are examples of hydrophobic colloids.

Destabilization of charged particles in water occurs as a result of the type of chemical (usually inorganic salts) causing coagulation. These salt ions reduce the electrostatic repulsion between particles to such a extent that the particles aggregate. Because of the double layer of electrical charge surrounding a charged particle, this aggregation mechanism

is sometimes called double-layer compression. The selection of type and dosage of the chemical coagulant must be made by experimentation, most commonly with "jar tests." For this effort, 150 *ml* graduated beakers were primarily used to measure the volume of floc produced. Coagulation involves the reduction of this electrostatic repulsion, such that colloidal particles of identical materials may aggregate. Flocculation depends upon the presence of bridging compounds, which form chemically bonded links between colloidal particles and enmesh the particles in relatively large masses called floc networks.

Polyelectrolytes of both natural and synthetic origin may cause colloids to flocculate. Polyelectrolytes are polymers with a high formula weight, normally contain ionizable functional groups, are long enough for one end to adsorb onto one particle and the other end onto a second particle (bridging). Somewhat paradoxically, anionic polyelectolytes may flocculate negatively charged colloidal particles. The mechanism by which this occurs involves bridging between the colloidal particles by way of the polyelectrolytes anions. Strong chemical bonding has to be involved, since both the particles and the polyelectrolytes are negatively charged. The flocculation process induced by anionic polyelectrolytes is greatly facilitated by the presence of a low concentration of a metal ion capable of binding with the functional groups on the polyelectolyte. The positively charged metal ion serves to form a bridge between the negatively charged anionic polyelectrolytes and negatively charged functional groups on the colloidal particle surface. Acrylamide, polyacrylamides, polystyrene sulfonate, polyacrlyate, polyvinyl pyridium, and polyethylene amine are examples of synthetic polymers.

For a synthetic polyelectrolyte to function effectively, it must be released from its transported state to be available as a free dissolved and fully extended single molecule. Sophisticated modern polymers are supplied in solid form for reasons of economy and ease of transportation and storage with the solid having a particle size distribution around a centrally selected mean. Each particle is a hard packed tangle of long polymer chains similar to a ball of string. For the individual chains to be released they must firstly absorb water to begin to uncoil by hydrating and activating their repulsive ionic groups. Unfortunately, the wetted polymer on the outer surface of each particle forms initially into a highly viscous gel which resists the passage of the free water necessary for wetting the polymer in the center of the particle. Thus, this initial absorption of water is dependent on the particle size.